

# Benchmark Determination of Shuttle Orbiter Entry Aerodynamic Heat-Transfer Data

David A. Throckmorton\*

NASA Langley Research Center, Hampton, Virginia

Entry aerodynamic heat-transfer data were determined from the first flight of the Space Shuttle Orbiter. The convective heating rate data result from a rigorous mathematical analysis of one-dimensional, transient heat conduction within the orbiter thermal protection system (TPS) and reradiation from its surface during entry. Temperatures measured at the TPS surface during orbiter entry provide a surface boundary condition for the analysis. The rigorous mathematical treatment provides for a "benchmark" determination of in-flight convective heat-transfer rates. The source of the entry thermal data, the mathematical analysis technique, and the TPS thermal models are discussed. Typical convective heating rate data from the STS-1 mission are presented.

## Nomenclature

$c_p$	= specific heat
GMT	= Greenwich mean time
$k$	= thermal conductivity
NBS	= National Bureau of Standards
$q$	= heating rate
$q_{\text{conv}}$	= convective heating rate
$q_{\text{rerad}}$	= reradiated heating rate ( $\epsilon \sigma T_s^4$ )
STS	= Space Transportation System
$T$	= temperature
$T_s$	= surface temperature
$t$	= time
$x$	= depth dimension
$X/L$	= nondimensional body length
$\epsilon$	= emissivity
$\lambda$	= thickness
$\rho$	= density
$\sigma$	= Stephan-Boltzmann constant

## Introduction

THE opportunity presented by the Space Shuttle to obtain accurate heat-transfer data on an entry vehicle in flight, over repeated entries, is unprecedented in the history of spaceflight. Flight convective heat-transfer data can provide a "benchmark" against which to compare wind-tunnel results and the predictions of state-of-the-art flowfield computational techniques. Comparison of flight- and ground-derived results may allow for improvements in the current capability to accurately predict the total aerothermodynamic environment to which a winged, lifting entry vehicle is subjected during entry from near-Earth orbit.

During the orbital flight test missions of the Space Shuttle, the orbiter vehicle has an instrumentation system onboard which records vehicle systems performance data for the purpose of design verification. Included among the measured parameters are over 200 measurements of temperature at the aerodynamic surface of the orbiter's thermal protection system (TPS). The measured time histories of surface temperature, coupled with appropriate mathematical modeling of the thermal protection system at each measurement location, allow for determination of convective heating rates to the vehicle over the entire entry from Earth orbit.

A transient analysis of heat conduction within the TPS, and reradiation from its surface, is used to determine the convective heating rate to the TPS surface at each measurement location. The measured temperature data provide a surface boundary condition for the analysis. The analysis is a mathematically rigorous simulation of heat conduction within the TPS, and reradiation from its surface, in order to provide a "benchmark" determination of convective heating rate.

## Data Source

During the orbital flight test missions, the orbiter has an instrumentation system onboard, referred to as the development flight instrumentation (DFI). The DFI is comprised of over 4500 sensors, associated data-handling electronics, and recorder, which provide data to enable postflight certification of orbiter subsystems design. Included among the DFI are measurements of the orbiter's aerodynamic surface temperature at over 200 surface locations (Fig. 1). These measurements are obtained from thermocouples mounted within the TPS, in thermal contact with the surface coating.<sup>1</sup> (Details of surface thermocouple installation will be discussed later.) The DFI also includes in-depth temperature measurements within the TPS materials at about 20 locations.

Development flight instrumentation temperature data are recorded once each second throughout the time period of entry from Earth orbit. The measured surface temperature time histories provide the basis for the determination of convective heating rates.

## Data Analysis Technique

A one-dimensional, transient analysis of heat conduction within the TPS, and reradiation from the TPS surface, is used to determine convective heating rates. The measured temperature data provide a surface boundary condition for the analysis, which is illustrated schematically in Fig. 2. The particular analysis technique being used<sup>2</sup> was originally developed as a tool for analyzing and sizing TPS concepts in vehicle system and trajectory synthesis/optimization programs. It is directly applicable to multiple-layered, insulative, thermal protection systems such as that of the Shuttle Orbiter.

Bradley<sup>3</sup> modified the original numerical analysis software to allow its application to the orbiter data reduction problem. The boundary condition at the heated surface was modified such that the surface temperature could be specified. The in-flight-measured surface-temperature data provide this temperature information. A simple energy balance at the heated surface [Eq. (1)] then provides for determination of

Presented as Paper 82-0003 at the AIAA 20th Aerospace Sciences Meeting, Orlando, Fla., Jan. 11-14, 1982; submitted July 20, 1982; revision received Oct. 18, 1982. This paper is declared a work of the U.S. Government and therefore is in the public domain.

\*Aerospace Technologist, Aerothermodynamics Branch, Space Systems Division. Member AIAA.

the surface heat flux.

$$q = -k \frac{\partial T}{\partial x} + \rho c_p \lambda \frac{\partial T}{\partial t} + \epsilon \sigma T_s^4 \quad (1)$$

conduction  
into silica  
tile
heat  
capacity  
of surface  
layer
reradiation  
from  
surface

The finite-difference formulation of the heat conduction problem is implicit; the heating rate computation [Eq. (1)] is explicit.

#### Thermal Models

There are three configurations of the orbiter's thermal protection system which are instrumented with surface thermocouples. These configurations are referred to as high-temperature reusable surface insulation (HRSI), low-temperature reusable surface insulation (LRSI), and flexible reusable surface insulation (FRSI). Both HRSI and LRSI are comprised of high-purity amorphous silica fibers, ceramic bonded and fabricated into blocks or tiles. The tiles are bonded to a strain isolation pad (SIP), which is, in turn, bonded to the underlying structure. HRSI tiles are coated with a black borosilicate-glass coating which provides for efficient radiation of thermal energy. LRSI tiles are coated with a white borosilicate-glass coating which provides for low solar absorptance. FRSI is a Nomex felt material, coated with a white silicon elastomeric film with low solar absorptance. FRSI is fabricated in large sheets and bonded directly to the structure. Each TPS configuration and its corresponding data analysis thermal model are shown in Fig. 3.

The thermal model used in the analysis of heat transfer to HRSI and LRSI surfaces (Fig. 3a) treats the surface coating as an isothermal heat sink. The heat capacity of the heat sink is

equal to the product of the nominal thickness, density, and specific heat of the coating material at the measured temperature. The backface structure, SIP, and adhesive layers are also treated as a lumped heat sink. The FRSI thermal model (Fig. 3b) is similar to that used for HRSI and LRSI; however, the adhesive layer between the felt and the structure is modeled. The underlying structure is treated as a heat sink. For all thermal models, 40 finite-difference nodes are used. Thirty of the nodes are equally spaced within the top one-fourth of the tile or felt thickness. Ten additional nodes are equally spaced throughout the remaining material. Parametric studies have shown that this node spacing provides solution accuracy commensurate with the use of many more node points while minimizing computational costs.

#### Thermocouple Installation

The surface thermocouples in HRSI and LRSI tiles are installed in a "trench" at the aerodynamic surface of the tile prior to application of the glass coating. The trench has a maximum width and depth approximately equal to the diameter of the thermocouple wire. The thermocouple wire is not insulated. Following installation of the thermocouple, the tile is coated such that the thermocouple bead and the entire length of wire at the tile surface are in contact with the coating. The "surface" measurement is then actually made at the interface between the silica tile and the coating. This provides an excellent measure of true surface temperature, however, because the thermal conductivity of the silica is an order of magnitude less than that of the coating. The coating reacts to input heat transfer much like a thin skin with an adiabatic backface.

For FRSI, the silicon coating is applied to the felt material before installation of the thermocouple. Thermocouple installation is accomplished by cutting a thin slit in the surface coating and laying the thermocouple wires and bead in place. The area of installation is then covered with a "bandaid" of coating material to protect the thermocouple.

#### Thermal Model Data Base

Thermal model information for each of the 200-plus orbiter locations where surface temperature measurements are obtained is stored in a computerized data base. This data base contains information on TPS thermal model type (HRSI, LRSI, FRSI) and layer thicknesses. The thermal model type information provides pointers into tables which contain the thermophysical properties of each TPS material. These properties include emissivity of surface coatings, specific heats as a function of temperature, thermal conductivities as functions of both temperature and pressure, and material

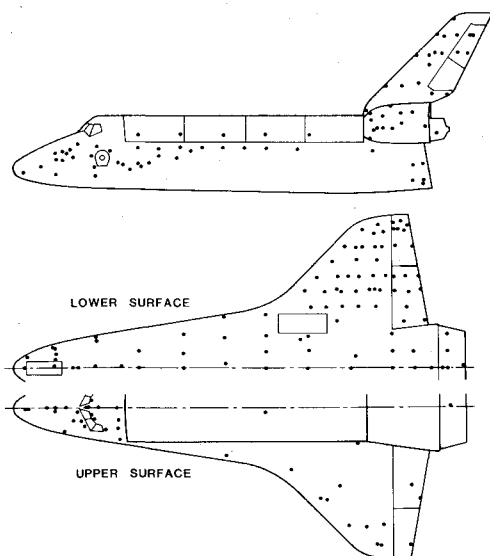


Fig. 1 DFI surface temperature measurement locations.

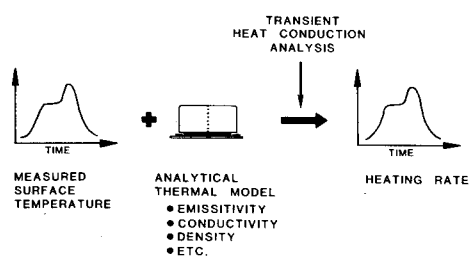


Fig. 2 Data analysis technique.

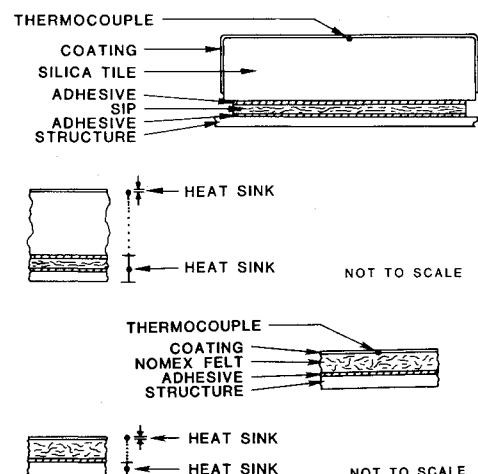


Fig. 3 TPS and TPS thermal model schematics: a) HRSI and LRSI; b) FRSI.

densities. The data analysis software uses the data base information to synthesize accurate mathematical thermal models at each location. The thermal model at each measurement location is unique because of the variation in TPS thickness about the vehicle and the multiple TPS types which are employed.

#### Data Processing System

Orbiter entry temperature data, in engineering units, are received on magnetic tape. These measured time histories of surface temperature are smoothed using a second-order, least-squares, curve-fit technique. The raw and smoothed data are then compared to assure that the smoothed data provide an accurate representation of the raw data. In cases where the smoothed data do not accurately represent the raw data, the smoothing parameters are modified and the data are reviewed interactively to obtain an accurate representation of the flight measured data.

Computation of convective heating rates is accomplished automatically using a data processing system developed specifically to operate on orbiter flight data. For each measurement location, the processing software queries the TPS thermal model data base, generates an accurate thermal model for that location, and reads the appropriate smoothed temperature data. The data are then processed by the thermal analysis software which determines convective heating rates.

#### Leeside Correction Factors

The data analysis technique being used to determine convective heating rates to orbiter surfaces assumes that all input energy is the result of convective heat transfer. However, on the leeside of the orbiter, where convective heating rates are very low, it is possible that a significant amount of the total energy input may result from solar radiation and, to the wing, cross radiation from the hot (relatively) orbiter fuselage. In order to account for the potential impact of these sources on the total energy input to leeside surfaces, values of solar- and cross-radiation heat-transfer rates are computed, based upon vehicle trajectory and attitude information and measured surface temperatures. These solar- and cross-radiation heating rate values are applied as "correction factors" to the total heating rate data in order to isolate the convective component of heat transfer. The technique used to compute these radiation heating rates and their significance as contributors to total leeside heat transfer are discussed in Ref. 4.

#### Uncertainty Assessment

The uncertainty of the convective heating rate data derived by the present method can be assessed by analyzing the surface energy balance of Eq. (1). The sensitivity of derived heating rates to uncertainties in any of the functional parameters has been previously assessed.<sup>3</sup> Because the thermal conductivity of the silica insulation is so low, the

energy balance is dominated, at high surface temperature, by the reradiative term  $\epsilon\sigma T_s^4$ . Therefore, the uncertainty of derived heating rate data is primarily influenced by the uncertainties of the measured temperature and the surface emissivity used in the data analysis.

#### Temperature

The end-to-end accuracy of the measured temperature data has been assessed by tracking the flow of temperature information from thermocouple output, through the onboard data-handling electronics, to the application of calibration data. This assessment considered the uncertainty in the EMF output of the thermocouples, the temperature stability of thermocouple reference junctions, the 8-bit word resolution of the DFI data-handling electronics, and the accuracy of curve fits to the calibration data. The root-sum-square uncertainty of measured temperatures is assessed to be less than  $\pm 2\%$  of reading at temperatures above 811 K (1000°F) for all vehicle windward surface measurements. Measurement uncertainty diminishes with increasing temperature. For measurements on leeside surfaces of the vehicle, the root-sum-square uncertainty of measured temperature is  $\pm 1.3\%$  of reading for LRSI surface temperatures above 811 K (1000°F) and FRSI surface temperatures above 533 K (500°F).

#### Emissivity

The derived heating rate data for HRSI surfaces to be presented in this paper have been generated using two disparate sets of surface emissivity information (Fig. 4). Both sets of emissivity data result from experimental measurements on baseline orbiter HRSI materials, but the measurement techniques are dissimilar.

Total hemispherical emittance data have been determined by D.A. Stewart of the NASA Ames Research Center using a "reflectance" measurement technique applied at room temperature. Spectral hemispherical emittance values were obtained from room-temperature reflectance data over the waveband from 0.27-15  $\mu\text{m}$ . Total hemispherical emittance as a function of temperature was then determined by integrating the room-temperature spectral emittance data across the waveband, in conjunction with the appropriate blackbody radiation spectra at elevated temperatures. The data determined by this method (Fig. 4) show an emissivity value of approximately 0.90 with minimal dependence upon temperature. These results have been independently verified by several other investigators using the same technique.

Total normal emittance data have also been determined by A.G. Kantios and S.F. Edwards of the NASA Langley Research Center using a "self-emission" measurement technique<sup>5</sup> at elevated temperatures. The self-emission measurement was accomplished by placing an HRSI sample and an NBS Inconel reference specimen in an oven and bringing them to a uniform, elevated temperature. A comparative measure was then made of the energy emitted by the HRSI sample and the Inconel standard over the waveband from 1-15  $\mu\text{m}$ , to determine the spectral normal emittance of the HRSI at the elevated temperature. The spectral emittance data, in conjunction with the blackbody radiation spectra at that temperature, were then integrated across the waveband to determine the total normal emittance of the HRSI. The data determined by this technique (Fig. 4) show a strong temperature dependence with emissivity decreasing from approximately 0.86 at room temperature to nearly 0.71 at 1300 K (1880°F).

The precision of either emittance measurement technique is considered herein to be of the order of  $\pm 6\%$ . The substantial difference in emissivity values at elevated temperatures, as determined by the differing techniques, is not understood. It is reported herein because of its critical importance to the determination of heat-transfer rates from flight-measured surface temperature data.

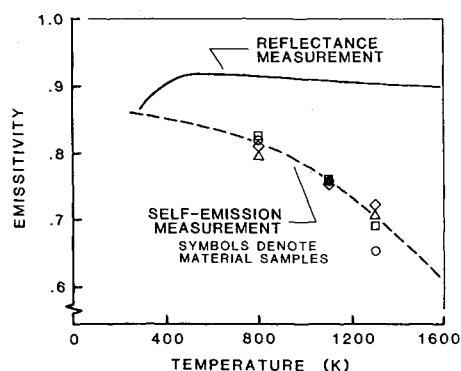


Fig. 4 HRSI surface emissivity.

Emissivity values for both LRSI and FRSI surfaces have also been determined by both the reflectance and self-emission techniques. Comparisons of these data show similar trends as observed for the HRSI. Quantitatively, the differences are not so dramatic, however, as maximum temperature levels are substantially lower.

#### Convective Heating Rate

It is assumed that the uncertainty in convective heating rate determined by the present method is a function only of uncertainties in the measured temperature, surface emissivity, and surface coating thickness. Other potential sources of uncertainty (for example, material specific heats, thermal conductivities, etc.) do not contribute significantly to the overall heating rate uncertainty.<sup>3</sup> The uncertainties of measured temperature and surface emissivity have been previously discussed. The uncertainty of the surface coating thickness is assessed to be  $\pm 31\%$  for HRSI,  $\pm 26\%$  for LRSI, and  $\pm 23\%$  for FRSI, based on TPS manufacturing specifications. Although the uncertainty in convective heating rate varies with surface temperature, time rate-of-change of temperature, and the spatial temperature gradient at the surface, the uncertainty may be nominally characterized as a function of surface temperature only, because of the dominance of the reradiative term. Assuming a  $\pm 6\%$  uncertainty in surface emissivity, the root-sum-square uncertainty in convective heating rate is assessed to be less than  $\pm 10\%$  at surface temperatures above 811 K ( $1000^\circ\text{F}$ ) for HRSI surfaces, less than  $\pm 9\%$  for LRSI surfaces above 533 K ( $500^\circ\text{F}$ ), and less than  $\pm 8.5\%$  for FRSI surfaces above 533 K ( $500^\circ\text{F}$ ).

#### STS-1 Results

The development flight instrumentation onboard data recorder did not operate during entry on the STS-1 mission. Consequently, actual flight-measured temperature data from STS-1 are available only for that portion of the entry during which the orbiter was in communications contact with ground stations.<sup>†</sup> A small amount of data was telemetered through the Guam tracking station prior to the time the orbiter began to experience significant aerodynamic heating. Data were also obtained very late in the trajectory (altitude  $\approx 53$  km to touchdown), on the downside of the aerodynamic heating pulse (Fig. 5).

Typical STS-1 temperature data from the vehicle's windward centerline are shown in Fig. 6a. Note that both laminar and turbulent data were obtained. Because the data analysis technique being used requires a temperature history for the entire trajectory from a known initial condition to allow an instantaneous determination of convective heating rate, a method of "recovering" the lost data was required. For measurement locations where the boundary layer was known to be laminar when flight data were initially acquired, simulated data (constrained to fit the actual flight data) were used to fill the large data gap (Fig. 6b). The simulated data were generated by assuming the local heating rate at any location to be a constant fraction of the 1-ft-sphere reference heating rate, for the STS-1 trajectory, from the time of entry interface to the time at which the first flight data were obtained. This constant heating rate ratio assumption is plausible because the angle of attack of the vehicle was approximately constant at  $40^\circ$  throughout this portion of the entry and only laminar data were treated in this manner. Composite temperature-time histories, such as that shown in Fig. 6b, were then used to compute convective heating rates for that portion of the STS-1 entry below an altitude of 53 km and Mach 11 (after acquisition of flight data). The use of

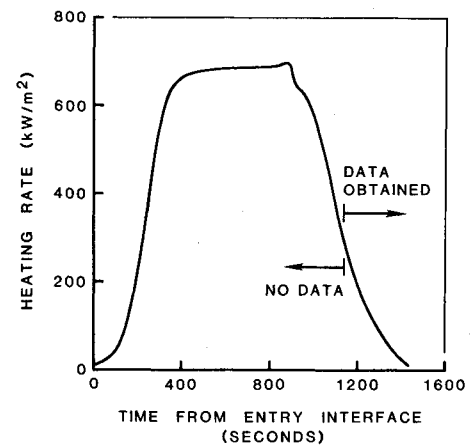


Fig. 5 STS-1 entry reference heating rate history.

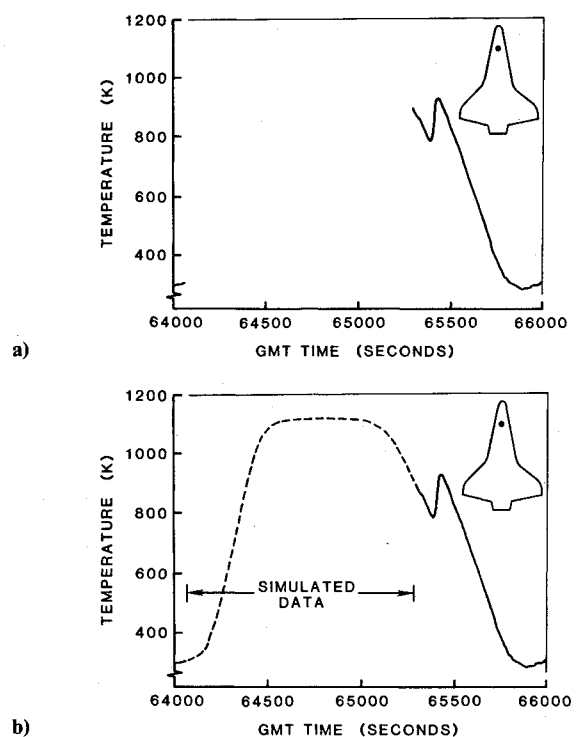


Fig. 6 Typical STS-1 surface temperature data: a) Flight data; b) simulated and actual flight data.

simulated surface temperature data allowed computation of the temperature distribution within the TPS at the time measured data were first obtained, thereby providing the required initial condition. Computed in-depth temperature distributions have been compared with measured in-depth temperatures and found to be in good agreement.

At the time of the first data acquisition, the boundary layer was laminar over approximately the forward 45% of the windward centerline. Convective heating rates were determined for that portion of the vehicle. Time histories of temperature and convective heating rate at several windward centerline measurement points are shown in Fig. 7 for the portion of the entry when measured data were available. The movement of the boundary-layer transition front past each measurement point is evidenced by the rapid increase and subsequent decrease in surface temperature. The rate of movement of transition from the aft portion of the vehicle to the nose may be determined by observing the time at which each measurement location experienced boundary-layer transition. The "double-maximum" evident in the heating

<sup>†</sup>A small amount of additional data was telemetered through an Air Force Advanced Range Instrumentation Aircraft (ARIA) which underflew the orbiter entry. These data are not considered in this paper, however.

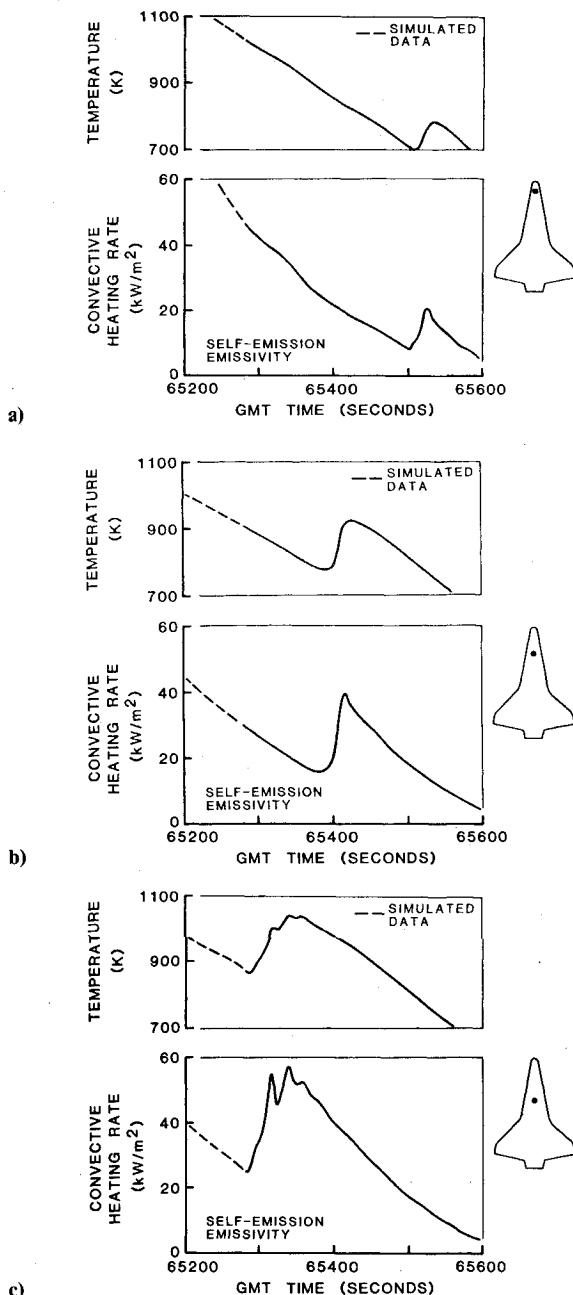


Fig. 7 STS-1 convective heating rate histories for points on the windward centerline: a)  $X/L = 0.09$ ; b)  $X/L = 0.24$ ; c)  $X/L = 0.38$ .

rate history as the transition front passed the  $X/L = 0.38$  measurement point (Fig. 7c), is typical of much of the transition data observed on STS-1.

Distributions of convective heating rate along the windward centerline are presented in Fig. 8 for three entry trajectory points. (The freestream flight environment for each of these trajectory points is defined in Table 1.†) Data are presented as determined by using the emissivity data obtained by both previously discussed measurement techniques. At the highest temperature levels, the difference in convective heating rate values determined using the two sets of emissivity data can be as large as 20% of the mean for the available STS-1 data. (The difference would be even larger for data obtained at maximum TPS temperatures.) As discussed in the companion paper (Ref. 8), the differing results obtained using the two sets

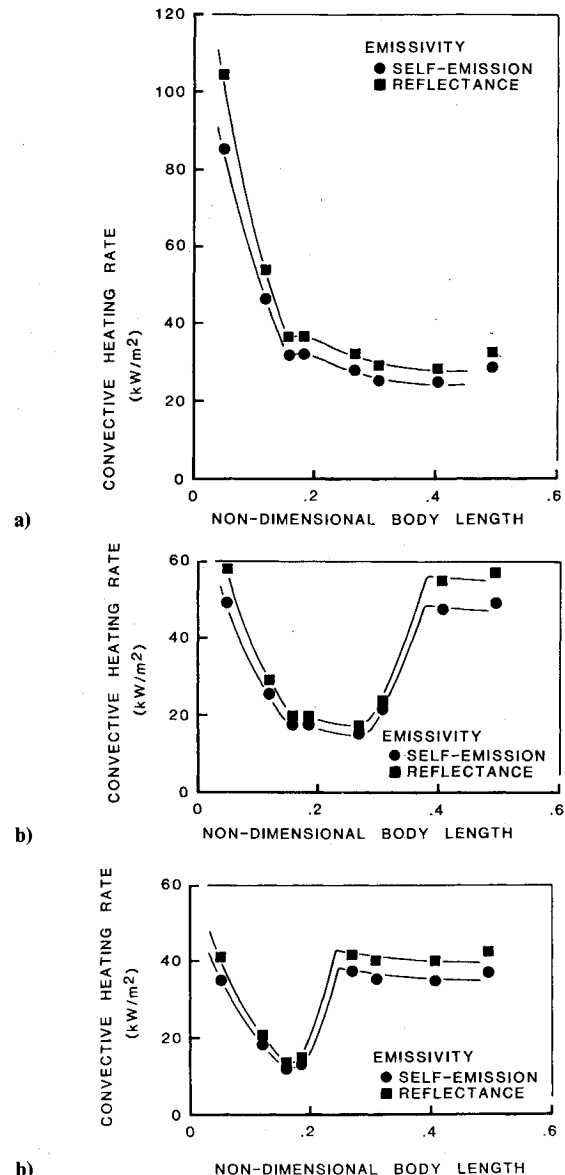


Fig. 8 STS-1 windward centerline convective heating rate distributions: a) GMT time = 65,280 s; b) GMT time = 65,375 s; c) GMT Time = 65,420 s.

of emissivity data can lead to widely differing interpretations of the STS-1 aerothermodynamic environment. Specifically, was the boundary-layer flow in chemical equilibrium, or was there a coupling of finite-rate chemistry in the flow with a TPS surface that was not fully catalytic in nature?

### Applicability of Present Technique

It is accepted engineering practice, when dealing with insulative thermal protection systems such as the orbiter's, to estimate convective heating rates, using measured surface temperatures, by assuming an adiabatic wall, radiation equilibrium energy balance at the surface. Convective heating rates are then determined by Eq. (2).

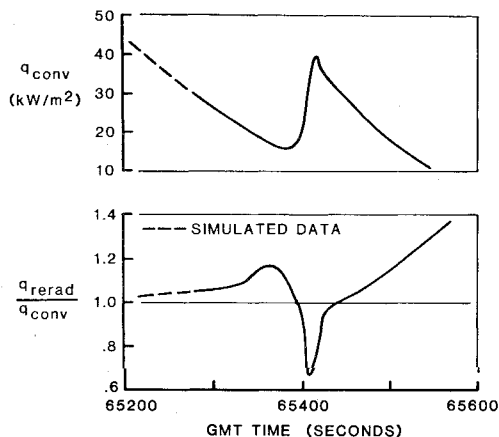
$$q_{\text{conv}} = q_{\text{rerad}} = \epsilon \sigma T_s^4 \quad (2)$$

Radiation equilibrium is an adequate approximation when heating rate levels are high and essentially steady state. The approximation breaks down, however, when the heating rate level is either low or changing rapidly with time. Under these circumstances, the TPS material heat capacity and thermal conductivity [i.e., the heat storage and conduction terms of

†The parameter values were determined by reconstruction of the entry trajectory, and the atmosphere along that trajectory, by the methods of Refs. 6 and 7, respectively.

Table 1 Entry flight environment definition

GMT time, s	Angle of attack, deg	Altitude, km	Velocity, m/s	Mach No.
65,280	39.2	52.9	3536	11.0
65,375	34.1	47.5	2640	8.1
65,420	30.8	44.2	2275	7.1

Fig. 9 Comparison of rigorous analysis results with radiation equilibrium approximation (windward centerline,  $X/L = 0.24$ , STS-1).

Eq. (1)] become important and a rigorous analysis technique is required for accurate determination of convective heating rate.

The importance of a rigorous analysis technique for STS-1 data may be qualitatively observed in the data of Fig. 7. Particularly note the "sharpness" of the maxima in the convective heating rate histories as the boundary layer becomes fully turbulent. If the TPS surface was adiabatic, in radiation equilibrium, the character of the temperature and heating rate curves would be identical. Quantitatively, in Fig. 9, the reradiated heating rate term, ratioed to the convective heating rate determined by the present method, is presented as a function of time for the data of Fig. 7b. The error in convective heating rate estimated by assuming radiation equilibrium can be extreme. The present analysis technique provides for accurate determination of convective heating rate regardless of heating rate level, and also when the heating rate is influenced by transient phenomena such as boundary-layer transition.

The ability to "track" transient phenomena can allow for assessment of convective heating rates to the orbiter at attitudes and control-surface configurations different from the nominal, by analyzing data from appropriate short-period, transient maneuvers. Hodge et al.,<sup>9</sup> have coupled a rigorous heat-conduction-analysis technique with maximum likelihood estimation logic to provide such a capability.

### Summary and Conclusions

A rigorous, one-dimensional mathematical analysis of heat conduction within the Shuttle Orbiter's thermal protection

system and reradiation from its surface, based upon in-flight measured temperatures, has been used to determine convective heating rates to the orbiter during the STS-1 entry. The analysis process has been automated to provide efficient processing of data from any of the more than 200 points on the orbiter surface at which thermal instrumentation is located. On the vehicle leeside, where heating rate levels are low, corrections are made to the computed convective heating rates to account for solar radiation and cross radiation between fuselage and wing surfaces.

TPS surface emissivity is one of the most important parameters used in the analysis process. However, of all the required parameters, its value is the most uncertain. Heating-rate data for STS-1 were derived using two disparate sets of measured emissivity data. One set was determined by a reflectance measurement technique, the other by a self-emission technique. The substantial differences in emissivity values observed at elevated temperatures, as determined by the differing techniques, are not understood. Derived heating rate levels for STS-1 differ as much as 20% depending upon the emissivity data used. If the uncertainty in the value of emissivity was reduced to  $\pm 6\%$ , the uncertainty in heating rates derived using the present method would be less than  $\pm 10\%$ , based upon the measurement uncertainties of the key parameters used by the analysis (e.g., emissivity, measured temperature, etc.).

The present method provides for a benchmark determination of convective heating rates, based upon in-flight measured temperature data. The method is accurate regardless of heating rate level and is capable of "tracking" changes in heating rate which result from transient events such as passage of the boundary-layer transition front or vehicle aerodynamic maneuvers.

### References

- <sup>1</sup>Stoddard, L.W. and Draper, H.L., "Development and Testing of Development Flight Instrumentation for the Space Shuttle Thermal Protection System," *Proceedings of the 24th International Symposium*, Instrument Society of America, 1978.
- <sup>2</sup>Pittman, C.M. and Brinkley, K.L., "One-Dimensional Numerical Analysis of the Transient Thermal Response of Multilayer Insulative Systems," NASA TM X-3370, 1976.
- <sup>3</sup>Bradley, P.F. and Throckmorton, D.A., "Space Shuttle Orbiter Flight Heating Rate Measurement Sensitivity to Thermal Protection System Uncertainties," NASA TM 83138, 1981.
- <sup>4</sup>Throckmorton, D.A., "Influence of Radiant Energy Exchange on the Determination of Convective Heat Transfer Rates to Orbiter Leeside Surfaces During Entry," AIAA Paper 82-0824, June 1982.
- <sup>5</sup>Edwards, S.F., Kantsios, A.G., Voros, J.P., and Stewart, W.F., "Apparatus Description and Data Analysis of a Radiometric Technique for Measurements of Spectral and Total Normal Emissivity," NASA TM D-7798, 1975.
- <sup>6</sup>Compton, H.R., Findlay, J.T., Kelly, G.M., and Heck, M.L., "Shuttle (STS-1) Entry Trajectory Reconstruction," AIAA Paper 81-2459, Nov. 1981.
- <sup>7</sup>Price, J.M. and Blanchard, R.C., "Determination of Atmospheric Properties for STS-1 Aerothermodynamic Investigations," AIAA Paper 81-2430, Nov. 1981.
- <sup>8</sup>Zoby, E.V., "Comparisons of Free-Flight Experimental and Predicted Heating Rates for the Space Shuttle," AIAA Paper 82-0002, Jan. 1982.
- <sup>9</sup>Hodge, J.K., Phillips, P.W., and Audley, D.R., "Flight Testing a Manned Lifting Reentry Vehicle (Space Shuttle) for Aerothermodynamic Performance," AIAA Paper 81-2421, Nov. 1981.